Original Article

Ionizing Radiation Promotes Epithelial-Mesenchymal Transition Phenotype and Stem Cell Marker in The Lung adenocarcinoma: *In Vitro* and Bioinformatic Studies

Mehdi Raei, Ph.D.[1], Mahdi Bagheri, Ph.D.[2], Safieh Aghaabdollahian, Ph.D.[3], Masoud Ghorbani, Ph.D.[4*], Afshin Sadeghi, M.Sc.[2]

1. Health Research Center, Life Style Institute, Baqiyatallah University of Medical Sciences, Tehran, Iran
2. Student Research Committee, Baqiyatallah University of Medical Sciences, Tehran, Iran
3. Department of Nanobiotechnology, New Technologies Research Group, Pasteur Institute of Iran, Tehran, Iran
4. Applied Biotechnology Research Center, Baqiyatallah University of Medical Sciences, Tehran, Iran

**Corresponding Address: P.O.Box: 19395-5487, Applied Biotechnology Research Center, Baqiyatallah University of Medical Sciences, Tehran, Iran*
Email: yasin.ghorbani93@gmail.com

Received: 31/December/2021, Accepted: 16/April/2022

Abstract

Objective: Ionizing radiation (IR) is one of the major therapeutic approaches in the non-small cell lung cancer (NSCLC); however, it can paradoxically result in cancer progression likely through promoting epithelial-mesenchymal transition (EMT) and the cancer stem cell phenotype. Therefore, we aimed to determine whether IR promote EMT/CSC and to investigate the clinical relevance of EMT/CSC hallmark genes.

Materials and Methods: In this experimental and bioinformatic study, A549 cell line was irradiated with a high dosage (6 Gy) or a fractionated regimen (2 Gy/day for 15 fractions). The EMT-related features, including cellular morphology, migratory and invasive capacities were evaluated using scratch assay and transwell migration/invasion assays. The mRNA levels of EMT-related genes (*CDH1, CDH2, SNAI1* and *TWIST1*), stemness-related markers (*CD44, PROM1,* and *ALDH1A1*) and the *CDH2/CDH1* ratio were evaluated via real-time polymerase chain reaction (PCR). The clinical significance of these genes was assessed in the lung adenocarcinoma (LUAD) samples using online databases.

Results: Irradiation resulted in a dramatic elongation of cell shape and enhanced invasion and migration capabilities. These EMT-like alterations were accompanied with enhanced levels of *SNAI1, CDH2, TWIST1, CD44, PROM1*, and *ALDH1A1* as well as an enhanced *CDH2/CDH1* ratio. *TCGA* analysis revealed that, *TWIST1, CDH1, PROM1* and *CDH2* were upregulated; whereas, *CD44, SNAI1* and *ALDH1A1* were downregulated. Additionally, correlations between *SNAI1-TWIST1, CDH2-TWIST1, CDH2-SNAI1*, and *ALDH1A1-PROM1* was positive. Kaplan-Meier survival analysis identified lower expression of *CDH1, PROM1* and *ALDH1A1* and increased expression of *CDH2, SNAI1*, and *TWIST1* as well as *CDH2/CDH1* ratio predict overall survival. Additionally, downregulation of *ALDH1A1* and upregulation of *CDH2, SNAI1* and *TWIST1* could predict a shorter first progression.

Conclusion: Altogether, these findings demonstrated that IR promotes EMT phenotype and stem cell markers in A549 cell line and these genes could function as diagnostic or prognostic indicators in LUAD samples.

Keywords: Dose Fractionation Lung Neoplasms, Epithelial-Mesenchymal Transition, Neoplastic Stem Cells, Radiotherapy

Cell Journal(Yakhteh), Vol 24, No 9, September 2022, Pages: 522-530

Citation: Raei M, Bagheri M, Aghaabdollahian S, Ghorbani M, Sadeghi A. Ionizing radiation promotes epithelial-mesenchymal transition phenotype and stem cell marker in the lung adenocarcinoma: in vitro and bioinformatic studies. Cell J. 2022; 24(9): 522-530. doi: 10.22074/cellj.2022.8403.

Introduction

Lung cancer is one of the most common cancers worldwide that leads to the highest number of cancer mortality. Lung cancer accounts for one-quarter of all cancer deaths (1). Non-small-cell lung cancer (NSCLC) is regarded as the main type of lung cancer, 85% of cases (2). In spite of the improvement in the survival rate of most cancers, the 5-year survival rate is 5% of lung cancer cases with distant stage disease (1). This low rate of survival could be due to intrinsic or acquired resistance to treatments, including radiotherapy and chemotherapy. Thus, it is necessary to define the molecular mechanism of such resistance and also, exploit potential agents to improve the lung cancer patient survival.

Ionizing radiation (IR), is classified as a main treatment strategy for patients with lung cancer. Various efforts such as dose escalation and altered fractionation have been done to improve the outcome (3). However, the results are inconclusive owing to various obstacles such as radioresistance. Emerging results demonstrated that epithelial-mesenchymal transition (EMT) can lead to the development of therapy resistance in lung cancer (4-6). EMT is a fundamental program that contributes to physiological events including embryogenesis and wound healing or human pathology including fibrosis and tumorigenic process. During EMT, an epithelial cell loses its traits such as epithelial junction and instead develops mesenchymal features including elongation of cytoplasm and nucleus, enhanced motility and invasive capacities. Moreover, EMT phenotype that contributes to the migration and invasion of tumor cells, also promotes the tumor cell dissemination from a primary site to secondary distant sites, and overrides chemotherapy- or radiotherapy-induced apoptosis (7). These changes are

regulated by EMT-core transcriptional factors which include SNAIL, TWIST, and zinc-finger E-box-binding (ZEB) families (8). For example, SNAIL and TWIST1 suppress the expression of genes linked to the epithelial phenotype such as *CDH1* (encoding E-cadherin) and concurrently promote the expression of genes linked to the mesenchymal phenotype such as *CDH2* (encoding N-cadherin). Moreover, the activation of EMT enables tumor cells to acquire stem-like properties, termed cancer stem cell (CSC) state. Enforced expression of EMT-master transcription factors such as SNAIL or TWIST in the epithelial cells induces the CSC phenotype development linking EMT phenotype with CSC state. These CSC subpopulations are defined using cell-surface markers such as CD44 and CD133 or via functional regulator of stemness such as ALDH (7).

Studies indicated that IR can lead to the EMT phenotype in the NSCLC cell lines (5, 6). Also, the induced changes were linked with enhanced radioresistance (5). A study showed that dose escalation might improve the survival rate of patients (9); while another report indicated that dose escalation not only did not improve the survival rate but also could likely be harmful (3).

A recent study documented that fractionation of irradiation (5 or 10 fractions of 2 Gy given one fraction per day) could induce EMT phenotype in the A549 human NSCLC cell line but not in the HT-29 human colorectal adenocarcinoma cell line (6). Induction of EMT phenotype that is recently envisioned to be the main cause of radioresistance might be impaired using higher dose or higher fractions of IR. In this study, we aimed to determine whether a higher dose or higher fractions of IR could induce EMT phenotype. Furthermore, the clinical significance of EMT and CSC-related genes was identified.

Materials and Methods

Cell culture

In this experimental and bioinformatic study, the human NSCLC cell line, A549, was obtained from National Cell Bank of Iran (NCBI). The cells were maintained in the Dulbecco's modified eagle's medium (DMEM, Gibco, Grand Island, NY, USA). The culture medium was completed via 10% (v/v) fetal bovine serum (FBS, Gibco, Grand Island, NY, USA), and 1% (v/v) penicillin/streptomycin. The cultured cells were incubated at 37ºC in a humidified 5% CO_2 environment. The present study was conducted with the approval of the Ethical Committee of the Baqiyatallah University of Medical Sciences, Tehran, Iran (IR.BMSU.REC.1399.414).

Irradiation

The A549 cell line was cultured in T25 flasks (Cat. No. 70025, SPL Life Sciences, Pocheon, South Korea). Once the cultured cells were more than 50-60% confluent, the cells were irradiated via a Varian linear accelerator (Varian Medical Systems, Palo Alto, CA, USA) with 6 MV energy and at a 2 Gy per min dose rate. The irradiation was performed with either a high dose of 6 Gy or a fractionated regimen consisting of a 2 Gy per fraction (five times/week) for 15 fractions (15 FR). Different analyses were carried out after 24 hours after the last irradiation.

Wound healing assay

Immediately, after the final irradiation, the cells were washed 3 times with phosphate buffered saline (PBS, Cat. No. BI-1401, Bioidea, Tehran, Iran) and digested by trypsin. Thereafter, the trypsin- digested cells were washed using PBS and resuspended in the complete medium. A sufficient number of cells ($\cong 5\times10^5$) were cultured into 6-well plates (Cat. No. 30006, SPL Life Sciences, Pocheon, South Korea) and allowed to adhere for 24 hours and reach confluency. The control (non-irradiated) cells were treated identically to the irradiated cells. The cell monolayer was scratched in a straight line via a sterile 200 µL pipette tip. To remove cell debris, the cells were washed with DMEM. Culture medium (DMEM) supplemented with 1% FBS was added and incubated in a 5% CO_2 environment at 37ºC. This FBS percentage was used to minimize the effect of cell proliferation on the assessment of migration. The wounded areas were captured through a microscope with 10x magnification at 0, 18, and 36 hours after wounding. The images were analyzed using ImageJ MRI-Wound-Healing-Tool (National Institutes of Health, Bethesda, Maryland, USA).

Transwell migration and invasion assays

The migratory capacity of irradiated and control cells was determined via transwell migration assay using 24-well transwell inserts (Cat. No. 35224, SPL Life Sciences, Pocheon, South Korea). The cells were seeded in the serum-free medium on the upper side of the porous membrane (8 µm pore size) of transwell insert. The transwell insert was placed in the lower well that was filled with 650 µL complete medium and incubated for 24 hours at 37ºC in a 5% CO_2 environment. The non-migrated cells were removed using a cotton swab, and the migrated cells were fixed and stained with methanol and crystal violet, respectively. The migrated cells were counted with ImageJ. Migration of cells was expressed as a relative migration which is calculated by percentage of a number of the migrated irradiated cells to the migrated control cells.

The invasive capacity of irradiated and control cells was evaluated via transwell invasion assay, which is carried out like transwell migration assay. Unlike transwell migration assay, the porous membrane must be pre-coated with matrigel (BD Biosciences, San Jose, CA, USA) in this assay. The invasion capability of the cells was expressed as relative invasion which is defined as percentage of invasion of the irradiated cells to invasion of control cells.

Real-time polymerase chain reaction

The mRNA levels of EMT and CSC markers were

evaluated via Quantitative real-time polymerase chain reaction (PCR). To this end, the total RNA extraction was carried out via RNeasy Plus-Mini Kit (Qiagen, Hilden, Germany). cDNA synthesis from 1 µg of the extracted-RNA from each treatment group was performed using QuantiTect Reverse Transcription Kit (Qiagen, Hilden, Germany). The real time qPCR analysis was set up via the QuantiNova SYBR Green PCR Kit (Qiagen, Hilden, Germany) and carried out in a LightCycler 96 System (Roche, Basel, Switzerland). The primer sequences were listed in a previous study (6). The primers with their melting temperatures (Tm), the accession number of the targeted refseq mRNA and length of the amplicon were provided in the Table S1 (See Supplementary Online Information at www.celljournal.org). The relative quantitation of gene expression was measured via the comparative CT (ΔΔCT) method and normalized to the HPRT gene. The Y- axis was represented as Log2 -transformed values.

Transcriptional expression and survival analysis using web tools

The relative expression of deregulated genes in human lung adenocarcinoma (LUAD) compared to normal samples was evaluated in The Cancer Genome Atlas (TCGA, http://cancergenome.nih.gov) using UALCAN (http://ualcan.path.uab.edu/) web tool. It should be noted that between the two predominant NSCLC histological phenotypes including adenocarcinoma and squamous cell carcinoma, we chose the adenocarcinoma because of our cell line. The analysis was carried out on 515 primary tumors of LUAD and 59 normal samples from TCGA. The expression of the gene of interest is provided as transcripts per million via Box and whisker plot. Moreover, the T-test was done via a PERL script with Comprehensive Perl Archive Network (CPAN) module "Statistics::TTest" (http://search.cpan.org/~yunfang/Statistics-TTest-1.1.0/TTest.pm) in order to evaluate the significance of difference in mRNA levels between primary tumors of LUAD and normal samples from TCGA (10). Additionally, the correlation among genes was evaluated in the LUAD samples from TCGA database using the gene expression profiling interactive analysis (GEPIA, http://gepia.cancer-pku.cn/) (11). The correlation coefficients (R value) were interpreted as follows: 0.00-0.1 indicates a negligible relationship; 0.1-0.39 indicates a weak relationship; 0.4-0.69 indicates a moderate relationship; 0.7-0.89 indicates a strong relationship; 0.9-1 indicates a very strong relationship (12).

The prognostic significance of the genes of interest in the human LUAD was evaluated using an online Kaplan-0Meier plotter (www.kmplot.com) which includes the microarray gene expression data and clinical survival data from the Cancer Biomedical Informatics Grid (caBIG, http://cabig.cancer.gov), the Gene Expression Omnibus (GEO, https://www.ncbi.nlm.nih.gov/geo/) and TCGA databases (13). According to the median value, the cases were classified into two risk groups, i.e. patient groups with higher or lower expression level of the gene of interest. The influence of differential gene expression on the overall survival (OS) and the first progression (FP) were determined via Kaplan-Meier curves. Of note, mean expression of the selected gene-probe sets was used when the prognostic value of metagene signatures was evaluated. Kaplan-Meier curves were provided with Hazard ratio (HR) and its 95% confidence intervals as well as log-rank P values. Moreover, $P<0.05$ were regarded to be statistically significant.

Statistical analysis

The statistical analysis was done via SPSS v.24.0 (SPSS, Inc., Chicago, IL). The Kolmogorov-Smirnov test was performed to evaluate whether the data was normally distributed. Mean differences between two groups were evaluated using the Independent t test, while, in the case of more than two groups, one-way analysis of variance (ANOVA) was carried out. A $P<0.05$ was regarded statistically significant. The data were shown as mean ± SD.

Results

Ionizing radiation changes cellular morphology

A previous study demonstrated that 2 Gy/day of fractionated radiotherapy for 5 or 10 days could promote EMT phenotype in the A549 cells (6); therefore, we aimed to evaluate whether higher fractions (15 fractions) or higher dose of IR could still induce EMT in the A549 cells (Fig.1A). As shown in Figure 1B, the morphology of irradiated A549 cells was significantly different in comparison with the control cells that did not receive any irradiation. Irradiation either fractionated (15FR) or high dose (6 Gy) resulted in a dramatic elongation of cellular shape and formation of membrane protrusions. These changes, which are characteristics of mesenchymal-like phenotype indicated that IR could promote EMT phenotype in A549 cell line.

Ionizing radiation enhances cell motility

Previous studies linked IR with enhanced cell motility. Based on the available data and morphological changes displayed above, we hypothesized that higher dose or higher fractions of IR could enhance cell motility. To evaluate this, we carried out a wound healing assay in which a wound was made in a confluent monolayer of control and irradiated cells (Fig.1C). As seen in Figure 1D, irradiated cells were able to refill the wounded area significantly faster than the control cells.

For A549-15 FR and A549-6 Gy cells, wound closure was 92.71% and 77.04% of the initial size after 36 hours,

respectively; whereas, for the control cells (no irradiation), wound closure was only 41.80% of the wounded area after 36 hours. This data indicated that irradiated cells had a higher motility than the control cells.

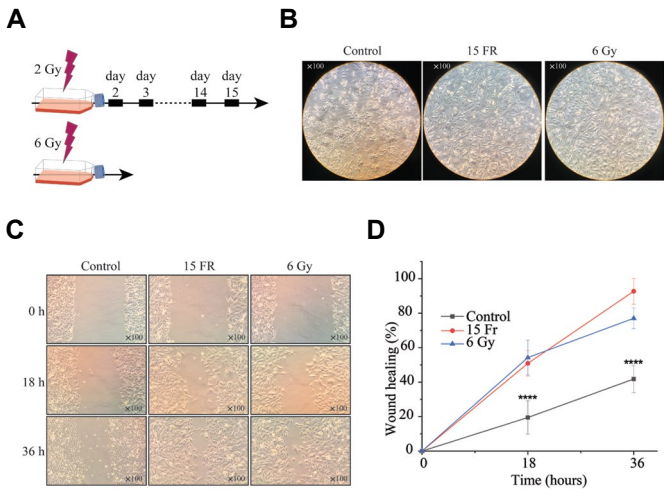

Fig.1: Ionizing radiation (IR) leads to morphological changes and enhanced migratory capacity of A549 cell line. **A.** Schematic representation of the cell line irradiation schedule. The A549 cells were irradiated with either a fractionated regimen comprising a 2 Gy fraction each day for 15 fractions (15 FR) or a single high dose of 6 Gy. **B.** Representative images of morphological alterations mediated by IR. **C.** Representative bright-field images showed that the scratches were enclosed faster in the irradiated cells. **D.** The motility of irradiated cells was statistically enhanced in comparison with the non-irradiated cells (****; P<0.001). The data were expressed as mean ± SD.

Ionizing radiation induces the migratory and invasive behaviors

EMT is featured with enhanced migratory and invasive capabilities (7). To further determine whether irradiated cells undergo EMT, we performed serum-promoted migration and invasion assays via transwell inserts. As represented in Figure 2A and B, A549-15 FR and A549-6 Gy cells migrated 46.67% (P=0.001) and 41.72%, respectively (P=0.004) that were migrated more than the non-irradiated cells through porous membrane. Moreover, the irradiated cells, A549-15 FR and A549-6 Gy, invaded 64.78% (P<0.001) and 45.18% (P=0.009) more than the parental cells through matrigel-coated membrane, respectively (Fig.2A). These results demonstrated that either higher fractions or higher dose of IR increased the migratory and invasive behaviors of the A549 cell line.

Ionizing radiation regulates EMT markers

To explore whether irradiation regulates the molecular changes consistent with EMT and CSC states, we performed RT-qPCR for several classic EMT/CSC marker genes. *CDH1*, an epithelial state marker, was not significantly downregulated in the A549-15 FR (P=0.665) and the A549-6 Gy (P=0.364); while, *CDH2*, the mesenchymal marker, was significantly upregulated in the A549-15 FR (P=0.024) and the A549-6 Gy (P<0.001, Fig.3A). The process of reduced expression of *E-CADHERIN* and increased expression of *N-CADHERIN* is referred to as 'Cadherin switch' which is considered as the EMT hallmark. We measured *CDH2* over *CDH1* ratio which could be an indicator of cadherin switch. This ratio in the A549-15 FR and the A549-6 Gy were approximately 10.59 (P<0.001) and 8.48 (P<0.001) folds higher, respectively, than in the control cells (Fig.3B), emphasizing the induction of EMT phenotype in the irradiated cells. Moreover, EMT related markers including *SNAI1* (A549-15 FR, A549-6 Gy, P<0.001) and *TWIST1* (A549-15 FR, P=0.036, A549-6 Gy, P<0.001) and CSC markers including *CD44* (A549-15 FR, A549-6 Gy, P<0.001), *PROM1* (A549-15 FR, A549-6 Gy, P<0.001) and *ALDH1A1* (A549-15 FR, P=0.036, A549-6 Gy, P<0.001) were significantly upregulated in irradiated cells.

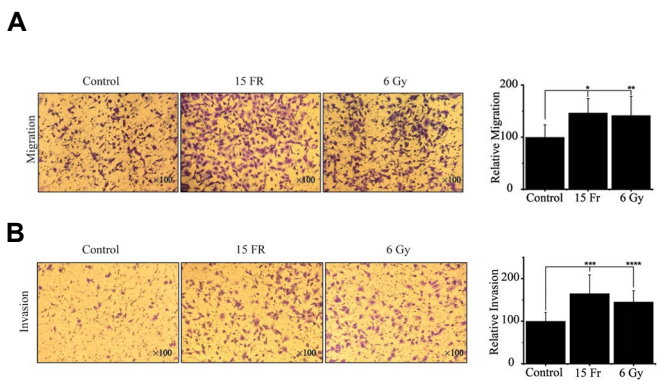

Fig.2: Ionizing Radiation (IR) increased the migratory and invasive capacities of A549 cell line. **A.** Microscopic images of migrated cells (on the left) and the analysis (on the right) showed the relative migration of A549-15 FR cells (*; P=0.001) and A549-6 Gy cells (**; P=0.004) was statistically more than that of non-irradiated cells. **B.** Microscopic images of migrated cells (on the left) and the analysis (on the right) showed the relative invasion of A549-15 FR cells (***; P<0.001) and A549-6 Gy cells (****; P=0.009) was statistically increased in comparison with the non-irradiated cells.

Transcriptional expression of deregulated genes in human LUAD

To further assess the clinical significance of our data, we analyzed the correlation of expression of EMT related genes with clinically relevant parameters. Using TCGA database, we first assessed the expression level of these genes in the human LUAD tumor tissues and compared with the normal non-cancerous tissues. Our analyses indicated that the expression of all seven genes was significantly altered in the tumor samples in comparison with the normal tissues (P<0.05). Consistent with their enhanced expression

in the irradiated A549 cells, *CDH2* (P<0.001), *PROM1* (P<0.001) and *TWIST1* (P<0.001) were statistically upregulated in the LUAD samples in comparison with the normal samples; while unlike cell line data, *CDH1* (P<0.001) was significantly upregulated and *CD44* (P<0.001), *SNAI1* (P=0.03), and *ALDH1A1* (P<0.001) were significantly downregulated in the tumor tissues (Fig.4A-G).

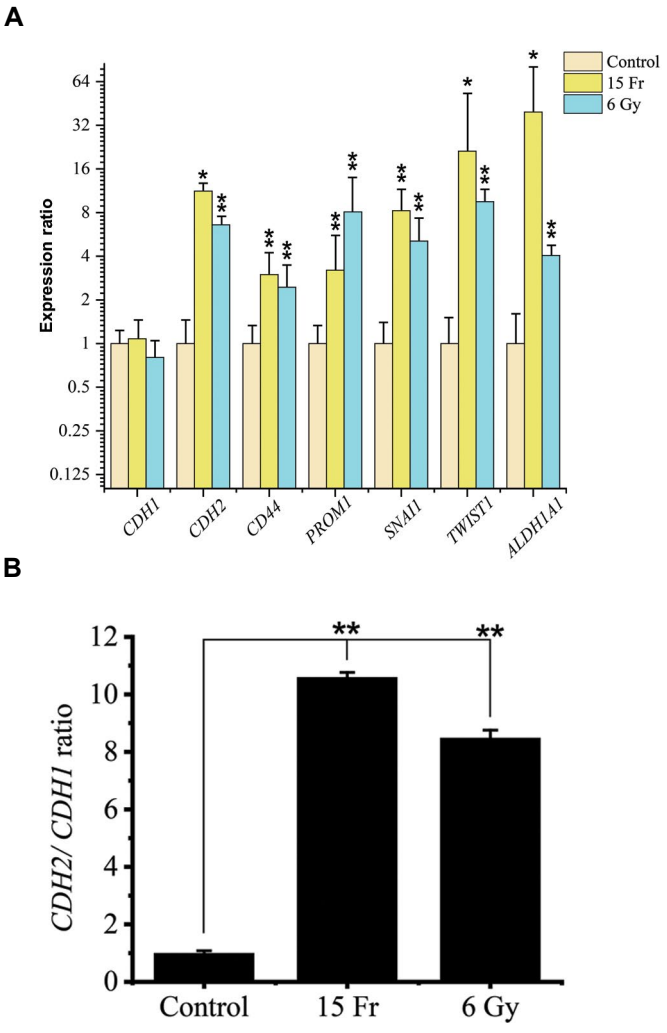

Fig.3: Ionizing radiation (IR) deregulated the expression of EMT related genes. **A.** The expression levels of *CDH2* (A549-15 FR: P=0.024, A549-6 Gy: P<0.001), *CD44* (A549-15 FR, A549-6 Gy: P<0.001), *PROM1* (A549-15 FR, A549-6 Gy: P<0.001), *SNAI1* (A549-15 FR, A549-6 Gy: P<0.001), *TWIST1* (A549-15 FR: P=0.036, A549-6 Gy: P<0.001) and *ALDH1A1* (A549-15 FR: P=0.036, A549-6 Gy: P<0.001) were significantly enhanced in the irradiated cells. **B.** The *CDH2* over *CDH1* ratio is enhanced (A549-15 FR, A549-6 Gy: P<0.001) in the irradiated cells in comparison with the non-irradiated cells. EMT; Epithelial-mesenchymal transition, *; P<0.05; and **; P<0.001.

Moreover, correlation among the EMT related genes was assessed in the LUAD samples from the TCGA using GEPIA. The analysis represented that there was a moderate and statistically significant correlation between *SNAI1* and *TWIST1* expression (R=0.48, P<0.001, Fig.4H). Moreover, the correlation between a pair of genes, including *CDH2-TWIST1* (R=0.36, P<0.001), *CDH2- SNAI1* (R=0.34, P<0.001), and *ALDH1A1-PROM1* (R=0.34, P<0.001) were weak but significant. However, the correlation among other genes was negligible (data not shown).

These data showed that the mRNA levels of EMT related genes are altered in primary lung cancer patient tissues, suggesting the potential importance of these genes in lung cancer development.

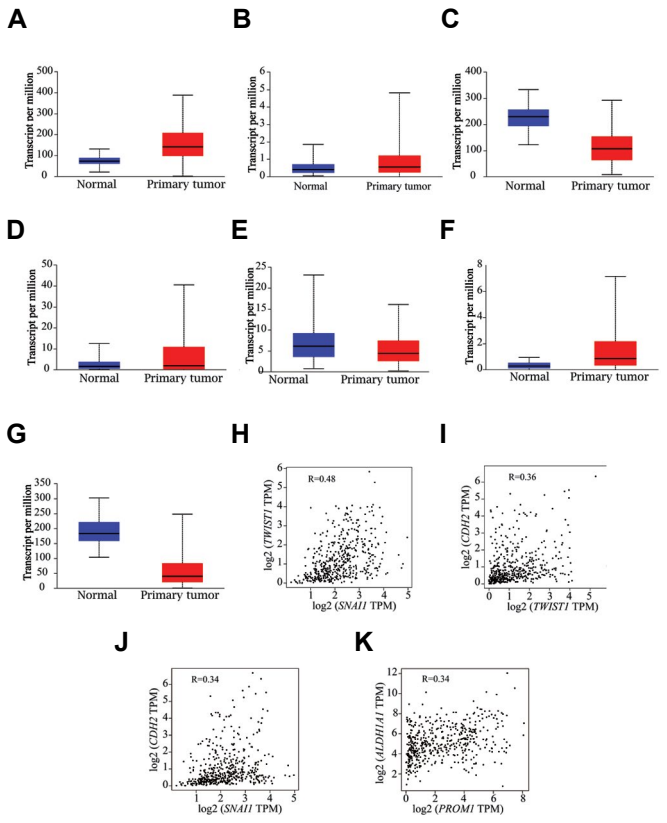

Fig.4: The expression of epithelial-mesenchymal transition (EMT) related genes was evaluated in the human lung adenocarcinoma (LUAD) tissues and the normal tissues deposited in the The Cancer Genome Atlas (TCGA) database. The analysis was carried out on the 515 primary LUAD tissues and the 59 normal samples. **A.** *CDH1* (P<0.001), **B.** *CDH2* (P<0.001), **C.** *CD44* (P<0.001), **D.** *PROM1* (P<0.001), **E.** *SNAI1* (P=0.03), **F.** *TWIST1* (P<0.001), **G.** *ALDH1A1* (P<0.001), **H.** *SNAI1* expression was associated with *TWIST1* expression in the LUAD patients (P<0.001). **I.** *TWIST1* expression was associated with *CDH2* expression in the LUAD patients (P<0.001). **J.** *SNAI1* expression was correlated with the *CDH2* expression in the LUAD patients (P<0.001). **K.** *PROM1* expression was associated with *ALDH1A1* expression in the LUAD patients (P<0.001).

Survival analysis of the deregulated genes in the human LUAD

Given the significant gene expression alterations of EMT related genes in the patient tumor tissues, we then assessed their association with survival rates of the LUAD patients. Survival analysis exhibited that

expression levels of *CDH1* (P=0.7), *CDH2* (P=0.85), *CD44* (P=0.45), *PROM1* (P=0.069), *SNAI1* (P=0.26), *TWIST1* (P=0.49), *ALDH1A1* (P=0.67), and Cadherin switch (P=0.7) did not statistically correlate with survival of the lung cancer patients who underwent radiotherapy (Fig.5).

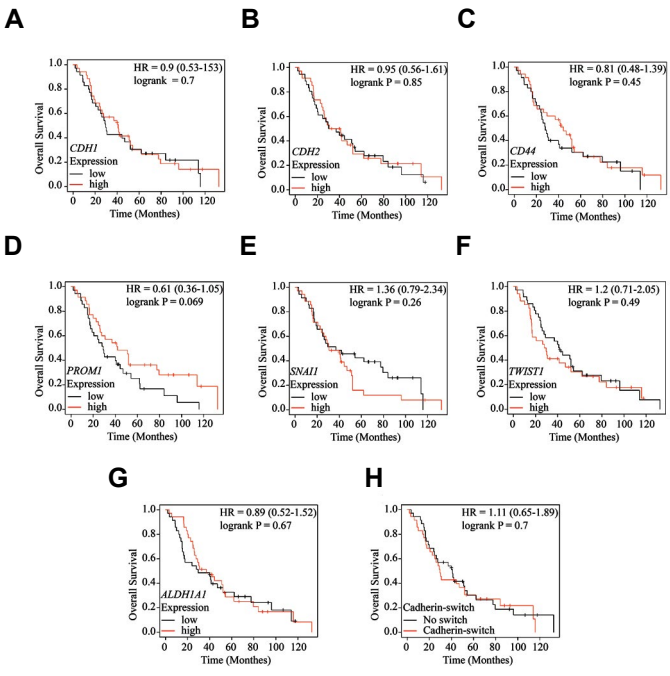

Fig.5: The overall survival (OS) lung adenocarcinoma (LUAD) patients who received radiotherapy was evaluated via the Cancer Biomedical Informatics Grid (caBIG), The Cancer Genome Atlas (TCGA) and GEO databases using the Kaplan–Meier plotter. **A.** *CDH1* (patients with high (35) and low (35) expression of *CDH1*; probe sets: 201130_s_at and 201131_s_at), **B.** *CDH2* (patients with high (34) and low (36) expression of *CDH2*; probe sets: 203440_at and 203441_s_at), **C.** *CD44* (patients with high (35) and low (35) expression of *CD44*; probe sets: 204490_s_at, 209835_x_at, 210916_s_at, 212014_x_at, 212063_at, 216056_at and 217523_at). **D.** *PROM1* (patients with high (35) and low (35) expression of *PROM1*; probe set: 204304_s_at). **E.** *SNAI1* (patients with high (35) and low (35) expression of *SNAI1*; probe set: 219480_at). **F.** *TWIST1* (patients with high (34) and low (36) expression of *TWIST1*; probe set: 213943_at). **G.** *ALDH1A1* (patients with high (35) and low (35) expression of *ALDH1A1*; probe set: 212224_at). **H.** Cadherin switch (Patients with cadherin switch (335) and no cadherin switch (35); probe sets: 201130_s_at, 201131_s_at, 203440_at and 203441_s_at).

Moreover, Kaplan-Meier analyses showed that elevated expression of *CDH2* (with HR=1.56 and P<0.001), *SNAI1* (with HR=1.41 and P=0.003) and *TWIST1* (with HR=1.31 and P=0.022) significantly correlated with decreased OS; whereas, decreased expression of *CDH1* (with HR=0.68 and P=0.001), *PROM1* (with HR=0.76 and P=0.02) and *ALDH1A1* (with HR=0.71 and P=0.004) significantly correlated with decreased OS (Fig.6). Moreover, the survival analysis of Cadherin switch (a subgroup in which *CDH1* is reduced and *CDH2* is enhanced) revealed that this combination was statistically correlated with reduced OS (HR=1.53, P<0.001) in LUAD patients (Fig.6H).

In the FP case, higher expression of *CDH2* (HR=1.88, P<0.001), *SNAI1* (HR=1.89, P<0.001) and *TWIST1* (HR=1.76, P<0.001) were significantly correlated with a shorter FP survival, while decreased expression of *ALDH1A1* (HR=0.59, P=0.001) was significantly correlated with a shorter FP survival (Fig.S1, See Supplementary On line Information at www.celljournal.org). Altogether, these data revealed the prognostic value of some of EMT related genes in lung cancer.

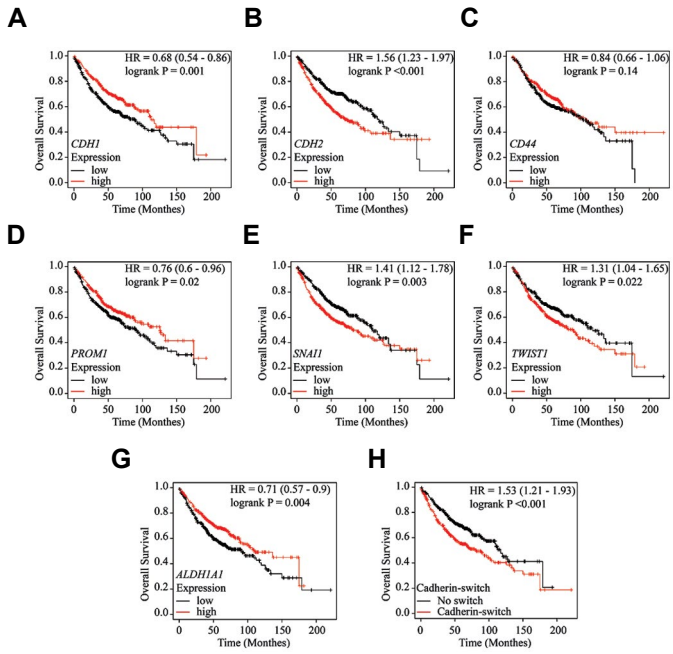

Fig.6: The overall survival (OS) of the lung adenocarcinoma (LUAD) patients was evaluated in the Cancer Biomedical Informatics Grid (caBIG), The Cancer Genome Atlas (TCGA) and GEO databases using the Kaplan–Meier plotter. **A.** *CDH1* (patients with high (359) and low (360) expression of *CDH1*; probe sets: 201130_s_at and 201131_s_at), **B.** *CDH2* (patients with high (359) and low (360) expression of *CDH2*; probe sets: 203440_at and 203441_s_at), **C.** *CD44* (patients with high (336) and low (336) expression of *CD44*; probe sets: 1557905_s_at, 204489_s_at, 204490_s_at, 209835_x_at, 210916_s_at, 212014_x_at, 212063_at, 216056_at and 217523_at). **D.** *PROM1* (patients with high (359) and low (360) expression of *PROM1*; probe set: 204304_s_at). **E.** *SNAI1* (patients with high (356) and low (363) expression of *SNAI1*; probe set: 219480_at). **F.** *TWIST1* (patients with high (359) and low (360) expression of *TWIST1*; probe set: 213943_at). **G.** *ALDH1A1* (patients with high (359) and low (360) expression of *ALDH1A1*; probe set: 212224_at). **H.** cadherin switch (patients with cadherin switch (359) and no cadherin switch (360); probe sets: 201130_s_at, 201131_s_at, 203440_at and 203441_s_at).

Discussion

Because of often asymptotic in the earlier stages, many cases of lung cancer patients were diagnosed at a distant stage. More than 50% of lung cancer at distant stage are treated with radiotherapy; however, the 5-year survival rate is 5% for these cases (14). Therefore, radiotherapy for these cases mainly remains palliative because of the intrinsic and/or acquired radioresistance (5). Identification of the mechanism and signaling pathway underlying such resistance might be crucial to find the therapeutic targets and develop novel therapeutic strategies to avert

radioresistance and eventually enhance the survival rate of patients. Recently, the radioresistance phenotype has been ascribed to a subset of tumor cells undergoing EMT (15). A previous study demonstrated that irradiation of 2Gy/day for 5 or 10 consecutive days promoted EMT phenotype in NSCLC cell line (A549) but not in the human colorectal adenocarcinoma cell line (HT-29). It was documented that higher fractions or higher doses of radiation are two strategies to improve radiotherapy outcome probably through reversing phonotypes that are ascribed to radioresistance such as EMT (16). Therefore, in the current study, we evaluated whether higher fractions or higher dosage of radiation could induce EMT in the NSCLC cell line, A549 Cell line. We observed that IR either fractionated or high dose could promote EMT phenotype in A549 cell line.

EMT is a complex program that enables epithelial cells to lose their features and acquire more mesenchymal features. Furthermore, EMT participates in the embryogenesis and the underlying mechanism is reactivated in the tumor progression and metastasis (7). Induction of EMT process regulates numerous aspects of cellular physiology, including cytoskeletal reorganization, cellular shape, loss of epithelial cell contacts, cellular polarity, development of cellular protrusions and induction of migratory and invasive capacities (17). These cellular changes are orchestrated via a cohort of transcription factors such as SNAIL, TWIST, and Zeb families (8). Many signals from tumor microenvironment have been identified that could lead to the EMT induction (18). In the current study, we also demonstrated that IR could promote morphological changes, including elongation of cellular shape, formation of membrane protrusions and loss of cell-cell interactions. These morphological changes were accompanied with enhanced motility of irradiated cells, a feature that plays a pivotal role in the cancer cell metastasis. Furthermore, the invasive capability of irradiated cells increased in comparison with non-irradiated cells. Accordingly, these findings were consistent with induction of Cadherin switch and enhanced the mRNA levels of mesenchymal markers (*CDH2*, *SNAI1* and *TWIST1*) and CSC marker (*CD44*, *PROM1* and *ALDH1A1*). These results were in consistence with previous findings that indicated that IR can induce an EMT state in the NSCLC cell lines (5, 19, 20). However, a previous study indicated that carbon ion irradiation inhibits the invasive capacity of the A549 cell line, demonstrating that carbon ion irradiation is more effective than photon irradiation in the suppressing the metastatic abilities of A549 cells (21). In the current study, we demonstrated that IR could induce Cadherin switch. During this switch, the transitioning cells tend to contact with mesenchymal cells instead of epithelial cells. However, the contacts between mesenchymal cells are weaker since the interaction between the homotypic *N-CADHERIN* is weaker than that of the homotypic *E-CADHERIN*. Thereby, Cadherin switch facilitates the motility and invasion (22, 23). Consistently, we showed that Cadherin switch is positively associated with the enhanced migration and invasion. As indicated, these processes are orchestrated by a set of transcription factors (22). Accordingly, we demonstrated that *TWIST1*, an EMT transcription factor that has emerged as a master regulator of the Cadherin switch (24-26), was significantly upregulated in the irradiated cells. After identification of the deregulated genes upon IR, their clinical relevance was evaluated using in silico approaches. The TCGA database composed 515 primary LUAD tumors and 59 normal samples. The TCGA database analysis revealed that *CDH1* was significantly upregulated in the LUAD samples. While, in vitro analysis indicated that IR did not statistically alter the *CDH1* expression in the NSCLC cell line and the reduced expression of *CDH1* predicted a poor prognosis of the LUAD patients. However, further studies are required to address the potential link between *CDH1* expression and prognosis of lung cancer patients who have undergone radiotherapy. In line with our irradiated *in vitro* model, *CDH2*, was significantly upregulated in the LUAD samples deposited in the TCGA database and this upregulation predicted a poor prognosis (both OS and FP) of LUAD patients. Cadherin switch could also predict the OS of the LUAD patients. The prognostic value of Cadherin switch was reported for prostate cancer and extrahepatic cholangiocarcinoma (27, 28). Given to the observed correlation between mRNA levels of *CDH2* and *TWIST1* in the LUAD and normal samples, the same trend was observed for *TWIST1*. Consistently, another study identified that either *CDH2* or *TWIST1* in primary NSCLCs was associated with a shorter OS (29). Altogether, these data indicated that these biomarkers might have diagnostic and/or prognostic values and targeting of which might be a therapeutic strategy, particularly in the case of LUAD that harbors an activating mutation in KRAS. Intriguingly, it was demonstrated that targeting of *TWIST1* has a synthetic lethal interaction with the frequently occurring *KRAS* mutation (30).

CD44 is mainly known as a CSC marker involving in the multiple aspects of metastasis, including proliferation, migration, invasion and radioresistance (31). A previous study, demonstrated that *CD44* is up regulated in the NSCLC cell line that undergone EMT and radioresistance phenotypes (6). While the bioinformatic analysis indicated that *CD44* is significantly downregulated in lung adenocarcinoma samples compared with normal tissues. These contradictory data indicate that radiotherapy might contribute in the induction of EMT or it might contribute in the selection of tumor cells undergoing EMT. In line with a meta-analysis (32), our bioinformatic data indicated that *CD44* expression did not significantly associated with OS and first progression. However, several studies indicated that *CD44* overexpression was associated with poor prognosis (33, 34); while, other studies demonstrated that downregulation of *CD44* was a poor prognostic factor demonstrating the dual role of *CD44* in cancer progression (35, 36). The dualistic role of *CD44* might be due to the cell lines variations, culture condition, tumor microenvironment, and evaluating *CD44* expression at

different stages of tumor progression (36). For example, hyaluronan (HA), one of the main elements of the ECM in the tumor microenvironment, in its high molecular weight could interact with *CD44* and promote formation of a complex among CXCL12, CD44 and CXCR4, that leads to angiogenesis and tumor metastasis, whereas low molecular weight hyaluronan could inhibit this complex formation (37). Additional controversies might be due to alternative splicing (38, 39). Alternative splicing of *CD44* generates two families of *CD44* isoforms, including: *CD44* standard isoform (*CD44*s) and variant isoforms of *CD44* (*CD44*v) (39). Recently, it has been identified that splice isoforms of *CD44* have opposite functions. *CD44*s is positively correlated with CSC/EMT gene signatures, while the *CD44*v shows an inverse correlation (38, 39). The *CD44*v is the major splice isoform in the epithelial state of tumor cells, however the *CD44*v expression switches to that of *CD44*s once the epithelial cells have undergone EMT or CSC phenotype. The *CD44* isoforms switching (*CD44*v to *CD44*s) is negatively regulated by ESRP1, a protein that is highly expressed in the epithelial cells (38, 39).

Conclusion

Altogether, these findings demonstrated that IR (either fractionated or high dose) could promote EMT in NSCLC cell line, A549 cell line, and EMT hallmark genes, particularly *CDH2* and *TWIST1*, could function as diagnostic or prognostic indicators in LUAD samples.

Acknowledgements

There is no financial support and conflict of interest in this study.

Authors' Contributions

M.R., M.B., M.G.; Contributed to conception and design. M.R., M.G., S.A., A.S.; Contributed to all experimental work, data and statistical analysis, and interpretation of data. M.G.; Overall supervision. M.G., S.A., A.S.; Drafted the manuscript. M.R., M.B.; Manuscript reviser. All authors read and approved the final manuscript.

References

1. Siegel RL, Miller KD, Jemal A. Cancer statistics, 2018. CA Cancer J Clin. 2018; 68(1): 7-30.
2. Chen Z, Fillmore CM, Hammerman PS, Kim CF, Wong KK. Non-small-cell lung cancers: a heterogeneous set of diseases. Nat Rev Cancer. 2014; 14(8): 535-546.
3. Bradley JD, Paulus R, Komaki R, Masters G, Blumenschein G, Schild S, et al. Standard-dose versus high-dose conformal radiotherapy with concurrent and consolidation carboplatin plus paclitaxel with or without cetuximab for patients with stage IIIA or IIIB non-small-cell lung cancer (RTOG 0617): a randomised, two-by-two factorial phase 3 study. Lancet Oncol. 2015; 16(2): 187-199.
4. Ghasemi Z, Tahmasebi-Birgani MJ, Ghafari Novin A, Motlagh PE, Teimoori A, Ghadiri A, et al. Fractionated radiation promotes proliferation and radioresistance in bystander A549 cells but not in bystander HT29 cells. Life Sci. 2020; 257: 118087.
5. Gomez-Casal R, Bhattacharya C, Ganesh N, Bailey L, Basse P, Gibson M, et al. Non-small cell lung cancer cells survived ionizing radiation treatment display cancer stem cell and epithelial-mesenchymal transition phenotypes. Mol Cancer. 2013; 12(1): 94.
6. Tahmasebi-Birgani MJ, Teimoori A, Ghadiri A, Mansoury-Asl H, Danyaei A, Khanbabaei H. Fractionated radiotherapy might induce epithelial-mesenchymal transition and radioresistance in a cellular context manner. J Cell Biochem. 2018; 120(5): 8601-8610.
7. Dongre A, Weinberg RA. New insights into the mechanisms of epithelial-mesenchymal transition and implications for cancer. Nat Rev Mol Cell Biol. 2019; 20(2): 69-84.
8. Ye X, Weinberg RA. Epithelial-mesenchymal plasticity: a central regulator of cancer progression. Trends Cell Biol. 2015; 25(11): 675-686.
9. Brower JV, Amini A, Chen S, Hullett CR, Kimple RJ, Wojcieszynski AP, et al. Improved survival with dose-escalated radiotherapy in stage III non-small-cell lung cancer: analysis of the National Cancer Database. Ann Oncol. 2016; 27(10): 1887-1894.
10. Chandrashekar DS, Bashel B, Balasubramanya SAH, Creighton CJ, Ponce-Rodriguez I, Chakravarthi B, et al. UALCAN: a portal for facilitating tumor subgroup gene expression and survival analyses. Neoplasia. 2017; 19(8): 649-658.
11. Tang Z, Li C, Kang B, Gao G, Li C, Zhang Z. GEPIA: a web server for cancer and normal gene expression profiling and interactive analyses. Nucleic Acids Res. 2017; 45(W1): W98-W102.
12. Schober P, Boer C, Schwarte LA. Correlation coefficients: appropriate use and interpretation. Anesth Analg. 2018; 126(5): 1763-1768.
13. Győrffy B, Surowiak P, Budczies J, Lánczky A. Online survival analysis software to assess the prognostic value of biomarkers using transcriptomic data in non-small-cell lung cancer. PLoS One. 2013; 8(12): e82241.
14. Miller KD, Siegel RL, Lin CC, Mariotto AB, Kramer JL, Rowland JH, et al. Cancer treatment and survivorship statistics, 2016. CA Cancer J Clin. 2016; 66(4): 271-289.
15. Krause M, Dubrovska A, Linge A, Baumann M. Cancer stem cells: Radioresistance, prediction of radiotherapy outcome and specific targets for combined treatments. Adv Drug Deliv Rev. 2017; 109: 63-73.
16. Moding EJ, Kastan MB, Kirsch DG. Strategies for optimizing the response of cancer and normal tissues to radiation. Nat Rev Drug Discov. 2013; 12(7): 526-542.
17. Shibue T, Weinberg RA. EMT, CSCs, and drug resistance: the mechanistic link and clinical implications. Nat Rev Clin Oncol. 2017; 14(10): 611-629.
18. Marcucci F, Stassi G, De Maria R. Epithelial-mesenchymal transition: a new target in anticancer drug discovery. Nat Rev Drug Discov. 2016; 15(5): 311-325.
19. Choi YJ, Baek GY, Park HR, Jo SK, Jung U. Smad2/3-regulated expression of DLX2 is associated with radiation-induced epithelial-mesenchymal transition and radioresistance of A549 and MDA-MB-231 human cancer cell lines. PLoS One. 2016; 11(1): e0147343.
20. Lu J, Zhong Y, Chen J, Lin X, Lin Z, Wang N, et al. Radiation enhances the epithelial- mesenchymal transition of A549 cells via miR3591-5p/USP33/PPM1A. Cell Physiol Biochem. 2018; 50(2): 721-733.
21. Ogata T, Teshima T, Inaoka M, Minami K, Tsuchiya T, Isono M, et al. Carbon ion irradiation suppresses metastatic potential of human non-small cell lung cancer A549 cells through the phosphatidylinositol-3-kinase/Akt signaling pathway. J Radiat Res. 2011; 52(3): 374-379.
22. Lamouille S, Xu J, Derynck R. Molecular mechanisms of epithelial-mesenchymal transition. Nat Rev Mol Cell Biol. 2014; 15(3): 178-196.
23. Theveneau E, Mayor R. Cadherins in collective cell migration of mesenchymal cells. Curr Opin Cell Biol. 2012; 24(5): 677-684.
24. Yang F, Sun L, Li Q, Han X, Lei L, Zhang H, et al. SET8 promotes epithelial-mesenchymal transition and confers TWIST dual transcriptional activities. EMBO J. 2012; 31(1): 110-123.
25. Yang MH, Hsu DS, Wang HW, Wang HJ, Lan HY, Yang WH, et al. Bmi1 is essential in Twist1-induced epithelial-mesenchymal transition. Nat Cell Biol. 2010; 12(10): 982-992.
26. Yang MH, Wu MZ, Chiou SH, Chen PM, Chang SY, Liu CJ, et al. Direct regulation of TWIST by HIF-1alpha promotes metastasis. Nat Cell Biol. 2008; 10(3): 295-305.
27. Araki K, Shimura T, Suzuki H, Tsutsumi S, Wada W, Yajima T, et al. E/N-cadherin switch mediates cancer progression via TGF-β-induced epithelial-to-mesenchymal transition in extrahepatic cholangiocarcinoma. Br J Cancer. 2011; 105(12): 1885-1893.
28. Gravdal K, Halvorsen OJ, Haukaas SA, Akslen LA. A switch from E-cadherin to N-cadherin expression indicates epithelial to mesenchymal transition and is of strong and independent importance for the progress of prostate cancer. Clin Cancer Res. 2007; 13(23):

7003-7011.
29. Hui L, Zhang S, Dong X, Tian D, Cui Z, Qiu X. Prognostic significance of twist and N-cadherin expression in NSCLC. PLoS One. 2013; 8(4): e62171.
30. Tran PT, Shroff EH, Burns TF, Thiyagarajan S, Das ST, Zabuawala T, et al. Twist1 suppresses senescence programs and thereby accelerates and maintains mutant Kras-induced lung tumorigenesis. PLoS Genet. 2012; 8(5): e1002650.
31. Chen C, Zhao S, Karnad A, Freeman JW. The biology and role of CD44 in cancer progression: therapeutic implications. J Hematol Oncol. 2018; 11(1): 64.
32. Jiang H, Zhao W, Shao W. Prognostic value of CD44 and CD44v6 expression in patients with non-small cell lung cancer: meta-analysis. Tumour Biol. 2014; 35(8): 7383-7389.
33. Hirata T, Fukuse T, Naiki H, Hitomi S, Wada H. Expression of CD44 variant exon 6 in stage I non-small cell lung carcinoma as a prognostic factor. Cancer Res. 1998; 58(6): 1108-1110.
34. Luo Z, Wu RR, Lv L, Li P, Zhang LY, Hao QL, et al. Prognostic value of CD44 expression in non-small cell lung cancer: a systematic review. Int J Clin Exp Pathol. 2014; 7(7): 3632-3646.
35. Leung EL, Fiscus RR, Tung JW, Tin VP, Cheng LC, Sihoe AD, et al. Non-small cell lung cancer cells expressing CD44 are enriched for stem cell-like properties. PLoS One. 2010; 5(11): e14062.
36. Louderbough JM, Schroeder JA. Understanding the dual nature of CD44 in breast cancer progression. Mol Cancer Res. 2011; 9(12): 1573-1586.
37. Fuchs K, Hippe A, Schmaus A, Homey B, Sleeman JP, Orian-Rousseau V. Opposing effects of high- and low-molecular weight hyaluronan on CXCL12-induced CXCR4 signaling depend on CD44. Cell Death Dis. 2013; 4(10): e819.
38. Zhang H, Brown RL, Wei Y, Zhao P, Liu S, Liu X, et al. CD44 splice isoform switching determines breast cancer stem cell state. Genes Dev. 2019; 33(3-4): 166-179.
39. Zhao S, Chen C, Chang K, Karnad A, Jagirdar J, Kumar AP, et al. CD44 expression level and isoform contributes to pancreatic cancer cell plasticity, invasiveness, and response to therapy. Clin Cancer Res. 2016; 22(22): 5592-5604.